Multiobjective Synthesis of a Polygeneration System for a Residential Building Integrating Renewable Energy and Electrical and Thermal Energy Storage

Edwin S. Pinto, Luis M. Serra

GITSE I3A, Department of mechanical engineering, University of Zaragoza, Spain

Abstract

The residential sector plays an important role in the action to combat climate change and its impacts. Recent studies show that the integration of thermal and electrical systems allows to increase the share of renewable energy, and the reduction of CO_2 emissions. Polygeneration systems lead to a reduction of economic costs and CO_2 emissions with respect to the separate production of energy services, thanks to an adequate systems integration. Achieving such benefits requires an appropiate design procedure bearing in mind that the minimization of the economic costs is often opposite to the minimization of the environmental impact. The aim of this paper is to carry out the synthesis of a polygeneration system for a residential building located in Zaragoza (Spain) encompassing renewable energy, thermal energy storage and batteries, considering economic and environmental aspects. A mixed integer linear programming (MILP) model has been developed to obtain trade-off solutions through the multiobjective optimization in two cases: grid connected and standalone systems. In both cases, five configurations of commercially available equipment were obtained, finding interesting solutions where significant CO_2 emissions reduction were achieved with a small increasing in the economic cost.

Keywords: Representative days, multiobejective optimization, polygeneration systems, MILP.

1. Introduction

A suitable energy process integration in polygeneration systems allows an effective way to achieve a lower consumption of natural resources, a reduction of CO_2 emissions and pollutant emissions as well as economic savings relative to conventional separate production (Mancarella, 2014). To achieve it, two fundamental issues must be addressed in the design of polygeneration systems (Pina et al., 2017; Wakui and Yokoyama, 2015): the synthesis of the plant configuration (installed technologies and capacities, etc.) and the operational planning (strategy concerning the operational state of the equipment, energy flow rates, purchase/selling of electricity, etc.). However, finding the optimal configuration of polygeneration systems in building applications is a complex task, given the wide variety of technology options available and great diurnal and annual fluctuations in energy demands and energy prices (Tapia-Ahumada et al., 2013). Additional factors that increase the complexity are: (i) the incorporation of renewable energy technologies, such as wind turbines, photovoltaic panels and solar thermal collectors, which are characterized by intermittent behavior and non-simultaneity between production and consumption; (ii) the incorporation of energy storage, either electrical and/or thermal, which allow to decouple production from consumption; and (iii) conflicting objectives, as the minimization of environmental and economic costs. Therefore, a MILP has been developed to tackle such issues focused in the multiobjective synthesis of a polygeneration system for a residential building located in Zaragoza (Spain) integrating electrical and thermal systems, driven by conventional and renewable energies for two cases: Grid connected and standalone systems. To do this, firstly, a set of representative days, in order to reduce the computational effort, is selected considering the energy demands, renewable energy production and CO_2 emissions, then the superstructure is defined considering the candidate technologies to cover the energy demands. Afterwards, the MILP model developed to carry out the multiobjective optimization is presented and finally, the trade-off solutions through the Pareto curve for both cases are analyzed.

2. Description of the system

A multifamily building composed of 12 dwellings, each one with 102.4 m^2 of surface area and an average occupancy of 3 people per dwelling located in Zaragoza-Spain is studied. The annual space heating SH_d, and

doi:10.18086/eurosun2018.11.02 Available at http://proceedings.ises.org

cooling R_d demands are respectively 49,889 kWh and 14,008 kWh, corresponding to 41 and 11 kWh/m^2 respectively according to IDAE (2009). Their hourly distribution is calculated by applying the *degree days* method and an hourly function distribution (Ramos, 2012). Heating degree days (HDD) and cooling degree days (CDD) are calculated with base temperatures $T_{bh} = 15$ ºC, for space heating and T_{bc}=21 ºC, for cooling. These values were selected as being suitable for Spain (Valor, E., Meneu, V., Caselles, 2001). Ambient temperature data (T_{amb}), and the required climatic data, are obtained from the *meteonorm* database (Meteotest, 2017). In the case of domestic hot water (DHW), the total annual consumption of 367.9 m^3 (IDAE, 2017), which is monthly distributed by applying a distribution factor (Viti, 1996). The energy required to heat the monthly volume of water is calculated considering the water network supply temperature (AENOR, 2005) and the required DHW temperature of 60 ºC established in the Spanish regulation (IDAE, 2017). Monthly energy is divided by days of the month and distributed by means of an hourly distribution function (Ramos, 2012). This procedure assumes that the hourly DHW energy demand Q_{DHW} is the same for every day of the month. In the case of electricity demand, the annual electricity demand for appliances and lighting is 35,267 kWh according to IDAE (2011a) which is monthly distributed by applying a distribution factor, which is divided by the days of the month and distributed by an hourly distribution function (Marín-Giménez, 2004), that considers different hourly consumption for each season, thus providing the hourly electricity demand E_d. The procedures briefly described above, provide the hourly demand data series of heating (Q_d), cooling (R_d) and electricity (E_d), where heating demand consists of space heating (SH_d) and DHW (Q_{DHW}).

Available renewable energy resources are calculated beforehand. Hourly energy production per square meter of photovoltaic, E_{PV}, and solar thermal, E_{ST}, are calculated using data manufacturers, according to the procedures described in (Duffie and Beckman, 2013). For photovoltaic technology PV, it has been considered polycrystalline modules of 255 Wp with the maximum point power efficiency η_{mp}=0.1566 and the temperature coefficient of open-circuit voltage μ_{Voc}=-0.32%/ºC (Atersa, 2017). In the case of solar thermal ST, collectors with optical efficiency $\eta_o = 0.801$, and 1st and 2nd order heat loss coefficients of a_1 =3.188 W/m^2·K, a_2 =0.011 W/m^2·K^2 (Salvador Escoda S.A, 2017). For both PV and ST, the production has been calculated as a function of the solar radiation G_T over a tilted surface at 36º and azimuth angle of 0º (Meteotest, 2017). Restriction due to shading is considered by applying the procedure described in (IDAE, 2011b). The area required to install PV and ST collectors is limited by the total area available in the multifamily building 400 m^2. For wind energy technology PW, the production E_{PW} has been calculated as a function of wind speed obtained from (Meteotest, 2017) and the production curve of a wind turbine of 3 kW of nominal capacity (Bornay, 2017) according to the procedure described in Manwell et al. (2009).

2.1 Selection of representative days

The timeframe of this case of study is one year, nevertheless, carrying out the optimization of dynamic energy systems by using hourly data for a whole year can become a computational demanding task, mainly when integer variables are involved. To tackle this issue, some strategies have been developed to define *representative days* (Domínguez-Muñoz et al., 2011; Poncelet et al., 2017), which allow to reproduce in a reasonable way the original data series of a whole year. To do this, every data series of energy demands and renewable energy production have to be considered simultaneously as well as CO_2 emissions data series (in particular for the hourly CO_2 emissions associated to the electricity consumed in the case of grid connected system) in order to match every hourly data considered in the optimization process. Hourly CO_2 emissions from the grid were collected from Red Electrica de España (2017) where are available in a time scale of 10 minutes; however, as the analysis is carried out hourly, it has been taken the average hourly to this study. Besides, year 2016 had 366 days so the 29 February data have not been considered. In the standalone system, data collection of CO_2 emissions is not required because these are only caused by the conventional equipment operation. In this study, we applied the *k*-medoid method (Domínguez-Muñoz et al., 2011) to select a set of twelve representative days (N_{rep}=12) to carry out the multiobjective optimization. Tab. 1 presents the representative days d along with their respective weights ω, which represents the number of times that has to be repeated *d* to approach to the original data series.

Tab. 1. Representative days

Month	*d*	*ω*	Month	*d*	*ω*	Month	*d*	*ω*
January	5	21	May	150	36	October	299	31
February	38	35	July	186	54	November	329	27
April	116	40	July	191	26	December	344	24
May	147	31	July	208	19	December	351	21

Scale factors were calculated and applied to the representative data to preserve the total energy demands, renewable energy production and CO_2 emissions from the original data series without exceeding the extreme values. In addition, normalized root-mean-square error (NRMSE) which represents the distribution of values and their frequency of occurrence for every duration curve were calculated in order to verify the accuracy of the representative data. The NRMSE has been calculated for each data series and it has been verified to be below 5%, which are considered appropriated in accordance with similar works such as Poncelet et al., (2017). On the other hand, two additional days corresponding to heating and cooling extreme demands are taken into account with weight zero in order to assure the coverage of the energy services in all circumstances, with the corresponding impact on the annual fixed cost, but not on the annual operation cost.

2.2 Superstructure definition including technical, economic and environmental data

The superstructure depicted in the Fig. 1, considers the candidate technologies and the feasible connections between them in the polygeneration system for both cases: grid connected and standalone. The system is composed of an electrical and thermal part. The electrical part consists of photovoltaic modules PV whose electrical production W_{PV} is a function of the modules area A_{PV}; wind turbines WT whose electrical production W_W is the result of the unit production E_{PW} multiplied by the number of turbines; inverter Inv which converts the direct current produced from renewable energy to alternating current, batteries Bat which can store electric energy and inverter-charger InvC which converts alternating current to direct current and conversely. The thermal part consists of conventional boiler GB that consumes fossil fuel F_b to produce heat; solar thermal collectors ST whose heat production Q_{ST} is a function of the area A_{ST}; a single-effect absorption chiller ACH that uses heat and a small quantity of electricity to produce cooling; and finally thermal energy storage for heating TSQ and cooling TSR, which can charge/discharge thermal energy. Components such as cogeneration module CM, converting the energy of fossil fuels F_c into electricity W_c and heat Q_c, and reversible heat pumps HP, converting the electrical energy E_{HP} into thermal energy either heating Q_{HP} or cooling R_{HP}, allow the integration of electric and thermal parts.

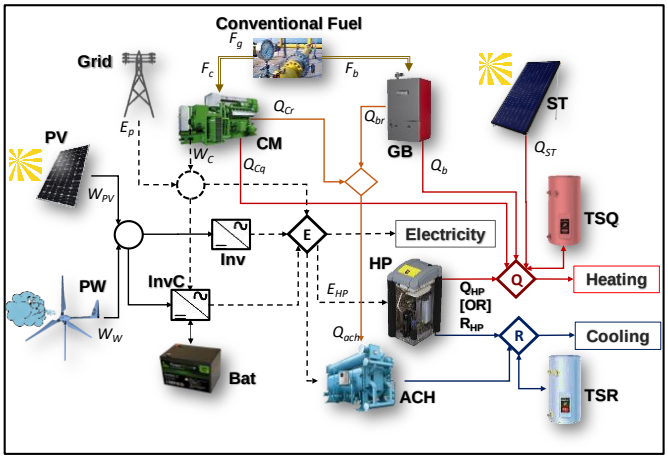

Fig. 1. Superstructure

From the point of view of operation, the electrical part considers a three-phase alternating current bus (ac-bus) with an operating voltage V_{ac} of 230 V and a direct current bus (dc-bus) with an operating voltage V_{dc} of 96 V with a maximum operating current $I_{max\text{-}dc}$ of 120 A. For the thermal part, a low temperature radiant heating indoor end system was considered, with operation temperatures about of 45 ºC, in addition, temperatures about 60 ºC are required for DHW. The required thermal energy for space heating and DHW can be provided by the heat pumps, solar thermal collectors, cogeneration module and boiler. In the case of cooling demands, temperatures of about 7-12 ºC are considered, and the required energy can be provided by the reversible heat pumps and the absorption chiller. The activation temperature for the absorption chiller is about 88 ºC, which thermal energy is produced in the boiler and/or the cogeneration module. Reversible heat pumps can operate in heating or cooling mode, but it is not allowed their operation simultaneously in both modes. The operation ranges of temperature and voltage are verified for all the components in the system according to manufacturers' catalogues.

Technical data

All technologies considered in the superstructure are commercially available. Main technical parameters obtained from the manufacturers' catalogues are shown in Tab. 2. The equipment can modulate up to nominal load, except

for the non-manageable ones (PV, ST and PW), cogeneration module CM and batteries. Heat pump operates in heating mode assuming a constant coefficient of performance COP, or in cooling mode assuming a constant Energy Efficiency Ratio EER with a constant cooling/heating capacity ratio β. Both COP and EER have been estimated considering the operational temperature of the reservoirs expected for Zaragoza (Spain). In the case of the CM, reciprocating engines are not allowed to work below 30% of the nominal capacity, and the electrical and thermal productions are proportional to α_w and α_q factors respectively. For the inverter and inverter-charger, an oversizing factor F_{inv} is applied to size their capacity, and efficiency η is applied to consider their performance. Single effect absorption chiller operates with a constant COP_{ACH}. The performance η_{GB} of conventional boiler is assumed constant. Regarding thermal energy storage tanks, the energy stored $S_q$and S_r for heating and cooling respectively, are calculated in each time step taking into account the energy losses by applying a λ factor. In the case of batteries, the round trip efficiency η_{rt}, determines the energy losses during the charging and discharging process in each time step. Charging and discharging processes are not allowed simultaneously either in thermal energy storage tanks or in batteries. Further, maximum deep of discharge DOD is defined for batteries to avoid premature failures. During the batteries lifetime operation, the number of charge-discharge cycles has to be lower than the maximum number of cycles that provoke the failure $N_{c,failure}$, indicated by the manufacturer. This is verified by applying the equivalent full cycle to failure ageing method described by Dufo-López et al. (2014). There are two technologies for batteries proposed for this study, ion lithium and lead acid, but in the optimal configuration, only one of them is selected. Models of capacity q, are applied to calculate their dynamic behaviour in the equipment. Ion lithium batteries capacity q_{ion}, are modelled according to DiOrio et al., (2015), taking into account both, the maximum charge current $I_{max,c}$ stablished by manufacturer and the charge ratio α_c in A/Ah described by Homer Energy (2016). For lead acid batteries, the technology used for this study is the OPz batteries applying the KiBaM model (Manwell and McGowan, 1993), which requires three parameters, calculated on the basis of manufacturers' data catalogues: k, the rate constant; c, the fraction of the capacity that may hold available charge; and the maximum capacity of the battery q_{max}, as a function of k and c. Taking into account that this study is based on representative days, for both, thermal and electrical storage, the energy stored at the beginning of each representative day must be equal to the energy stored at the end of each representative day.

Economic data

The investment cost of every component is calculated from the unit cost Cu and the installed capacity. Installation and maintenance costs are considered by applying the factor F_m. In order to calculate the fixed annual cost, a Capital Recovery Factor CRF=0.082 yr^{-1} is applied based on a lifetime of the installation of 20 years and an interest rate $r = 5\%$. However, some components have different lifetime n_r, hence, a net present value factor $FNPV$ is calculated for every component to consider the total repositions carried out during the lifetime of the installation. The indirect costs are considered by applying a factor F_{ind} of 0.2. For all investments, the Value-Added Tax VAT, is applied, whose value for Spain case is 0.21. All economic data are shown in Tab. 2.

In grid connected case, the polygeneration system has the possibility of selecting the required contracted power from the grid Pct below 15 kW, with a cost of cPct of 44.76 €/kW. A time-of-use tariff has been applied with three time periods with different cost of electricity purchased cp_i: i) 0.195302 €/kWh from 14 to 23 hours; ii) 0.123573 €/kWh at 1 hour, 24 hour and from 8 to 13 hours; and iii) 0.0091957 €/kWh from 2 to 7 hours. These tariffs apply for both winter and summer (Endesa, 2017). Also it has been considered a meter equipment rental cost C_{alq} of 16.32 €/yr and the electricity tax of Tax_e=0.05113.

The natural gas *NG* contract depends on annual gas consumption. For our study, the tariff 3.2, which annual consumption must be below 50,000 kWh/yr has been considered. This has a fixed cost C_{fg} of 101.4 €/yr and a constant price cp_{NG} of 0.04328 €/kWh (Endesa, 2017). Further, a meter equipment rental cost C_{alq-g} of 15 €/yr is considered. In the case of standalone system only gasoil for heating *GH* with fixed price cp_{GH} of 0.0613 €/kWh (Eurostat, 2017) has been considered.

Environmental data

In order to evaluate the environmental impact of the polygeneration system, it has been considered the unit CO_2eq emissions embodied CO_2U in every component of the superstructure based on the life cycle assessment *LCA* of every component (see Tab. 2), the CO_2 emissions released due to the natural gas combustion considering a constant value of 0.252 $kgCO_2eq/kWh$ (IDAE, 2016) and the hourly CO_2 emissions due to electricity consumption from the grid (Red Electrica de España, 2017). In the case of standalone system, CO_2 emissions released due to the gasoil combustion were calculated considering a constant value of 0.311 $kgCO_2eq/kWh$ (IDAE, 2016).

Tab. 2. Technical, economic and environmental data

Component j	Technical data	Economic data			Environmental data	References
		Cu [€/*]	Fm	n_r [Years]	CO_2U [kgCO_2eq/*]	
PV	η_{mp}= 15.66% μ_{Voc}=-0.32%/ºC	113.4 €/m²	0.5	20	161 kgCO_2eq/m²	(Ardani et al., 2016; Atersa, 2017; Frischknecht et al., 2015; Fthenakis and Raugei, 2017; JUDELSA, 2017)
PW	Manufacturer curve	6404 €/ud	2	20	2160 kgCO_2eq/ud	(Bornay, 2017; Orrell and Poehlman, 2017; Tremeac and Meunier, 2009)
ST	$\eta_o = 0.801$ a_1 =3.188 W/m²K a_2 =0.011 W/m²K²	254 €/ m²	1.5	20	95 kgCO_2eq/m²	(Guadalfajara, 2016; IDAE, 2011c; SALVADOR ESCODA S.A, 2017)
GB	η_b: 0.96	80 €/kWt	0.5	15	10 kgCO_2eq/kWt	(BAXI, 2017; Pina et al., 2017)
HP	COP=3.0, EER= 4.0, β=0.9	500 €/kW	0.5	20	160 kgCO_2eq/kWt	(Beccali et al., 2016; ENERTRES, 2017; Pina et al., 2017)
ACH	COP_{ACH}= 0.7	485 €/kWt	1.5	20	165 kgCO_2eq/kWt	(Beccali et al., 2016; Pina et al., 2017; U.S. Department of Energy, 2017)
CM	α_w= 0.28,α_q= 0.56	1150 €/kW	0.7	10	65 kgCO_2eq/kWe	(Darrow et al., 2017; Pina et al., 2017)
TSQ	λ= 1%	376 €/kWh	0.1	15	31 kgCO_2eq/kWht	(BAXI, 2017; Beccali et al., 2016; ISSF, 2015)
TSR	λ= 3%	752 €/kWh			62 kgCO_2eq/kWht	
Bat Ion-Li	η_{rt}=90%; *DOD*=80%; $N_{c,failure}$ =8000;α_c=0.4	500 €/kWh	0.25	15	160 kgCO_2eq/kWh	(Cho et al., 2015; Parra et al., 2017; Peters et al., 2017)
Bat Lead Acid	η_{rt}= 70%; *DOD*=60%; $N_{c,failure}$=2000; *k*=0.11, *c*=0.53	220 €/kWh	0.25	7	60 kgCO_2eq/kWh	(Cho et al., 2015; Hiremath, Mitavachan & Derendorf, Karen & Vogt, 2015; McManus, 2012; Parra et al., 2017)
Inv	η_{inv}= 96%, η_{invc}= 94%, F_{inv}=1.2	400 €/kW	0.5	15	191 kgCO_2eq/kW	(Ardani et al., 2016; Frischknecht et al., 2015; Fthenakis and Raugei, 2017; Fu et al., 2017; JUDELSA, 2017)
InvC		774 €/kW	0.25	15	191 kgCO_2eq/kW	

3. Optimization model

A MILP model is developed using the software LINGO (LINDO Systems Inc, 2013) to carry out the multiobjective optimization. The two objective functions are: economic and environmental cost. In the case of the economic cost the objective is to minimize the total annual cost (eq. 1), consisting of the investment annual cost CIA, and operational costs C_{op}.

$$MIN = CIA + C_{op} \quad \text{(eq. 1)}$$

$$CIA = (1 + VAT) \cdot (1 + F_{ind}) \cdot CRF \cdot \sum_{j=component} Cu_j \cdot Cap_j \cdot \left(1 + FNPV_j\right)\left(1 + F_{m_j}\right) \quad \text{(eq. 2)}$$

$$C_{op} = C_E + C_g \quad \text{(eq. 3)}$$

In the grid connected system the operational cost is composed of the annual electricity purchased cost C_E (eq. 4) (sell to the grid is not allowed) and the annual natural gas purchased cost C_g. The first term C_E, has a fixed cost C_f (eq. 5) as a function of the contracted power from the grid Pct, which must be greater than the electricity purchased E_p in any time t (eq. 6) and a variable cost C_v calculated by (eq. 7) according to time-of-use tariff and the weight of each representative day ω_d.

$$C_E = \left(\left(C_f + C_v\right) \cdot (1 + Tax_e) + C_{alq}\right) \cdot (1 + VAT) \quad \text{(eq. 4)}$$

$$C_f = cPct \cdot Pct \quad \text{(eq. 5)}$$

$$Pct\ (t) \geq Ep(t) \quad \text{(eq. 6)}$$

$$C_v = \sum_{d=1}^{N_{rep}} \omega_d \cdot (\sum_{t=1}^{24} cp_i(t) \cdot Ep(t))_d \quad \text{(eq. 7)}$$

The annual gas purchased cost is calculated by (eq. 8). This is composed of two fixed costs namely, C_{fg} and C_{alq-g}, and a variable cost C_{vg} (eq. 9) which is proportional to the natural gas consumption F_{NG}. In the case of standalone system there is not electricity consumption from the grid and C_g refers only to the annual gasoil consumption in which there is not fixed cost associated, but variable cost C_{vg}which is proportional to the gasoil consumption F_{GH}.

$$C_g = \left(C_{fg} + C_{alq-g} + C_{vg}\right)(1 + VAT) \quad \text{(eq. 8)}$$

$$C_{vg} = \sum_{d=1}^{N_{rep}} \omega_d \cdot \left(\sum_{t=1}^{24} cp_{NG/GH} \cdot F_{NG/GH}(t)\right)_d \quad \text{(eq. 9)}$$

In the case of the environmental cost, the objective is to minimize the CO_2 emissions (eq. 10). The environmental objective function is composed of a fixed part $CO2_{fix}$ corresponding to the CO_2 emissions embodied in the components (eq. 11) and a variable part $CO2_{ope}$ corresponding to the CO_2 emissions due to the conventional fuel consumption and/or electricity consumption from the grid during the operation system (eq. 12).

$$MIN = CO2_{fix} + CO2_{ope} \quad \text{(eq. 10)}$$

$$CO2_{fix} = \sum_j CO_2U(j) \cdot CAP(j) \cdot \left(1 + Repl_j\right)/nyr \quad \text{(eq. 11)}$$

$$CO2_{ope} = \sum_{d=1}^{N_{rep}} \omega_d \cdot \left(\sum_{t=1}^{24}\left(CO2_{NG/GH} \cdot F_{NG/GH}(t) + CO2_{grid}(t) \cdot Ep(t)\right)\right)_d \quad \text{(eq. 12)}$$

$Repl$ is the number of replacements carried out during the lifetime of the installation for every component, $CO2_{NG/GH}$ is the CO_2 emissions associated to the combustion of the natural gas (grid connected system) or gasoil (standalone system) in $kgCO_2eq/kWh$, and $CO2_{grid}(t)$ are the CO_2 emissions associated to the electricity from the grid in each hour, in $kgCO_2eq/kWh$.

Both, economic and environmental cost functions are minimized subject to:

Balance equations:

An energy balance is carried out in each node m of the superstructure:

$$\sum_m (E_{in}^m - E_{out}^m) = 0 \quad \text{(eq. 13)}$$

Equipment efficiency:

GB: $\eta_{GB} \cdot F_b - Q_b = 0$ (eq. 14)

HP: $Q_{HP} - E_{HP} \cdot COP = 0$ (eq. 15)

HP: $R_{HP} - E_{HP} \cdot EER = 0$ (eq. 16)

CM: $\alpha_w \cdot F_c - W_c = 0$ (eq. 17)

CM: $\alpha_q \cdot F_c - Q_c = 0$ (eq. 18)

ACH: $R_{ach} = COP_{ach} \cdot Q_{ach}$ (eq. 19)

For each energy in-out through the inverter or inverter-charger *j*:

$$E_{out_j} - \eta_j \cdot E_{in_j} = 0 \quad \text{(eq. 20)}$$

For thermal energy storages for heating $_q$ and cooling $_r$:

$$S_{q,r}(t) = S_{q,r}(t-1) \cdot \lambda_{q,r} + E_{in_{q,r}} - E_{out_{q,r}} \quad \text{(eq. 21)}$$

For batteries the charge efficiency η_{ch}, and discharge efficiency η_{dis} are considered for the charge I_{ch} and discharge I_{dis} currents, and the charge $E_{b_{in}}$and discharge $E_{b_{out}}$energies:

$$\eta_{rt} = \eta_{ch} \cdot \eta_{dis} \quad \text{(eq. 22)}$$

$$E_{b_{in}}(t) \cdot \eta_{ch} - I_{ch}(t) \cdot V_{dc} \cdot t = 0 \quad \text{(eq. 23)}$$

$$E_{b_{out}}(t) - \eta_{dis} \cdot I_{dis}(t) \cdot V_{dc} \cdot t = 0 \quad \text{(eq. 24)}$$

Equipment's capacities:

For renewable energy production components:

PV: $W_{PV} = E_{PV} \cdot A_{PV}$ (eq. 25)

ST: $Q_{ST} = E_{ST} \cdot A_{ST}$ (eq. 26)

PW: $W_W = E_{PW} \cdot N_{aer}$ (eq. 27)

For each component *j*, the energy production is equal or lower than its nominal capacity. Thus, for heating Q, cooling R or electricity W production:

$$Q_j \leq Cap_j \quad \text{(eq. 28)}$$

$$R_j \leq Cap_j \quad \text{(eq. 29)}$$

$$W_j \leq Cap_j \quad \text{(eq. 30)}$$

For thermal energy storage for heating and cooling:

$$S_{q,r} \leq Cap_{TSQ,TSR} \quad \text{(eq. 31)}$$

The capacity in kWh for batteries, is the product of the capacity q in kAh multiplying by V_{dc}:

$$q_{bat} \cdot V_{dc} \leq Cap_{bat} \quad \text{(eq. 32)}$$

The capacity of the inverter and inverter-charger must be greater than the sum of all energy fluxes into the devices in any time *t*. As aforementioned, an oversizing factor F_{inv} is applied:

$$F_{inv} \cdot \left(\sum_{j=Inv,InvC} E_{in_j}(t)\right) \leq Cap_j \quad \text{(eq. 33)}$$

4. Results and discussion

The multiobjective optimization is carried out for the two systems aforementioned: grid connected and standalone. For both systems, the two objective functions (economic and environmental) were evaluated separately as a first step. Reference systems based on conventional equipment were considered to evaluate the advantage of the use of polygeneration systems. In these reference systems, heat pump *HP* is used only for cooling. Afterwards, multiobjective optimization is carried out based on ε-constraint procedure to construct the Pareto curve.

4.1 Single Objective optimization

In the grid connected system, electricity from the grid and natural gas are available for the system. The reference scenario does not consider renewable energy, cogeneration module, absorption chiller and energy storage systems. Energy from the grid E_p covers the electricity demand E_d and can be used to run the heat pump only for cooling. Natural gas is available to be used in the boiler to cover heating demands. In the polygeneration system, only ion-lithium technology has been considered in the optimization of the superstructure.

Tab. 3 Grid connected system. Single optimization results

System	Polygeneration system		Reference system
Equipment	**Economic optimum**	**Environmental optimum**	
Grid contracted power [kW]	13.856	13.856	17.321/24.249/17.321
Cogeneration module CM [kW]	1.6	0.0	0.0
Photovoltaic modules PV [m^2]	68.7	75.0	0.0
Wind turbine PW [kW]	0.0	16.3	0.0
Solar thermal collectors ST [m^2]	0.0	85.9	0.0
Heat pump HP [kWt]	77.7	48.3	78.1
Gas boiler GB [kWt]	23.0	5.1	65.2
Absorption chiller ACH [kWt]	0.3	0.3	0.0
Heat thermal storage TSQ [kWht]	0.0	46.6	0.0
Cooling thermal storage TSR [kWht]	0.0	54.5	0.0
Batteries BAT [kWh]	0.0	13.1	0.0
Electricity consumption [kWh]	***24518***	***18444***	***38770***
Gas consumption [kWh]	***50000***	***122***	***72901***
Annual cost [€/yr]	***18444***	***45480***	***22565***
Annual CO_2 emissions [kgCO_2eq/yr]	***18307***	***6328***	***25658***

According to the values shown in Tab. 3, comparing the polygeneration system with respect to the reference systems, we observe that it could be achieved a reduction of about 18% and 29% in the annual cost and CO_2 emissions respectively from the economic optimum or it would be needed double the annual cost to achieve a reduction of about 75% in the annual CO_2 emissions from the environmental optimum. On the other hand, by using polygeneration systems, it is possible reduce the contracted power from the grid and natural gas, achieving a significant reduction in electricity and natural gas consumption.

In the standalone system, electricity from the grid and natural gas are not available. Therefore, gasoil for heating is used as a conventional fuel to run the boiler GB and the cogeneration module CM. This last, produce electricity

to cover the demand E_d and for running the heat pump HP as well. A reference system in which energy demands are attended only by cogeneration module, heat pump (only for cooling) and boiler is considered. In both systems, reference and polygeneration systems the thermal energy storage (TSQ and TSR) and batteries are considered to tackle the restriction of reciprocating engines to work above 30% of partial load. Both systems are optimized with lead acid (OPz) and ion-lithium (Ion-Li) batteries separately. Tab. 4 and Tab. 5 present the main results for both cases.

Tab. 4. Standalone system with ion lithium batteries. Single optimization results

Ion Lithium System	**Standalone polygeneration system**		**Standalone reference system**	
Equipment	**Economic optimum**	**Environmental optimum**	**Economic optimum**	**Environmental optimum**
Cogeneration module CM [kW]	6.9	7.2	14.9	10.6
Photovoltaic modules PV [m^2]	91.5	149.3	0.0	0.0
Wind turbine PW [kW]	0.0	45.0	0.0	0.0
Solar thermal collectors ST [m^2]	0.0	11.5	0.0	0.0
Heat pump HP [kWt]	48.9	65.8	77.0	32.9
Gas boiler GB [kWt]	36.6	0.0	52.0	44.1
Absorption chiller ACH [kWt]	26.3	10.1	0.0	0.0
Heat thermal storage TSQ [kWht]	0.0	77.3	0.0	45.3
Cooling thermal storage TSR [kWht]	0.0	1.0	1.0	97.3
Batteries BAT [kWh]	1.3	60.0	17.6	6.8
Annual Fuel consumption [kWh]	***105449***	***22501***	***170673***	***163781***
Annual cost [€/yr]	***22998***	***71056***	***29358***	***38189***
Annual CO_2 emissions [kgCO_2eq/yr]	***34588***	***13480***	***54289***	***52223***

Tab. 5. Standalone system with Lead Acid batteries. Single optimization results

Lead Acid System	**Standalone polygeneration system**		**Standalone reference system**	
Equipment	**Economic optimum**	**Environmental optimum**	**Economic optimum**	**Environmental optimum**
Cogeneration module CM [kW]	6.9	7.5	14.7	9.3
Photovoltaic modules PV [m^2]	93.0	148.0	0.0	0.0
Wind turbine PW [kW]	0.0	45.0	0.0	0.0
Solar thermal collectors ST [m^2]	0.0	12.8	0.0	0.0
Heat pump HP [kWt]	47.8	65.1	77.0	26.6
Gas boiler GB [kWt]	37.2	0.0	46.1	41.9
Absorption chiller ACH [kWt]	27.2	10.5	0.0	0.0
Heat thermal storage TSQ [kWht]	0.0	83.9	0.0	53.2
Cooling thermal storage TSR [kWht]	0.0	1.3	1.0	126.6
Batteries BAT [kWh]	1.0	78.3	24.0	9.3
Annual Fuel consumption [kWh]	***106364***	***23527***	***173442***	***163693***
Annual cost [€/yr]	***23040***	***70639***	***29215***	***41573***
Annual CO_2 emissions [kgCO_2eq/yr]	***34871***	***13528***	***55083***	***52291***

From the comparison between the polygeneration systems with respect to the reference system, we can observe a reduction of about 20% and 35% in the annual cost and CO_2 emissions respectively from the economic optimum, and an increasing of about 70% in the annual cost to achieve a reduction of about 75% in the annual CO_2 emissions from the environmental optimum.

4.2 Multiobjective optimization

In order to carry out a multiobjective optimization, a Pareto solution's set are found by means the ε-constraint method (Haimes et al., 1971) . This means that we can obtain different solutions by optimizing one of the objective functions whereas the value of the other objective function is fixed. This procedure can be carried out as many times as required to create the Pareto curve. The solutions in between the single-objective optimization solutions are known as trade-off solutions or non-dominated solutions. For both systems, five different configurations through the Pareto curves were defined according to the minimum capacities commercially available.

Fig. 2a shows the Pareto curve of the grid connected system. Along the curve different solutions are obtained with different configurations and capacities. Each symbol corresponds to a specific configuration (with different pieces of equipment and capacities).

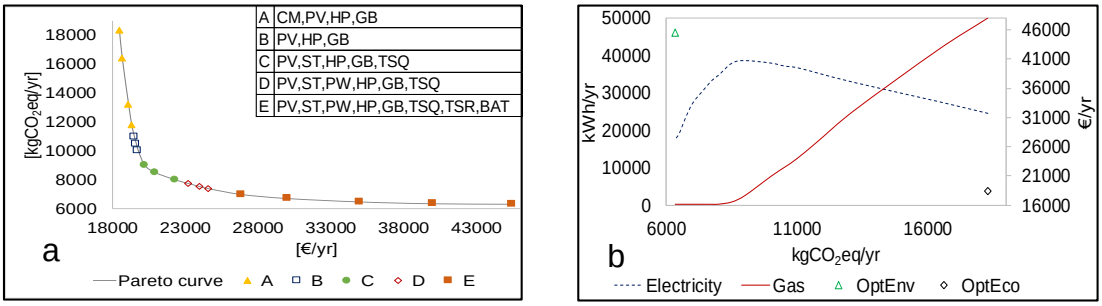

Fig. 2. a) Grid connected system Pareto curve. b) Electricity and gas consumption vs CO_2 emissions

There is not an absolute "best solution", because it depends on the decision maker. The set of Pareto solution's must be evaluated to take the "best solution" according to the weights of different objectives considered for the decision maker. For the authors, configurations B and C seem to be interesting trade-off solutions considering the great reduction of CO_2 emissions about 43% and 54%, with only an increasing of about 7% and 15% in the total annual cost respectively, with respect to the economic optimum. Configuration B is simpler than C, in fact is the simplest configuration among the Pareto curve configurations, therefore, could be considered the best trade-off solution considering its simplicity and their achievements in terms of the relation annual cost / CO_2 emissions.

On the other hand, Fig. 2b shows the electricity and natural gas consumption with respect to the CO_2 emissions. From the economic optimum (OptEco) to the environmental optimum (OptEnv) gas consumption always decrease whereas electricity consumption increases up to reach the maximum point at 9000 $kgCO_2eq/yr$, then it decreases rapidly, due to the PV and PW increasing capacity. The electricity is mainly use to run the heat pump to produce heating/cooling, which shows the advantage of using this technology to reduce the environmental impact.

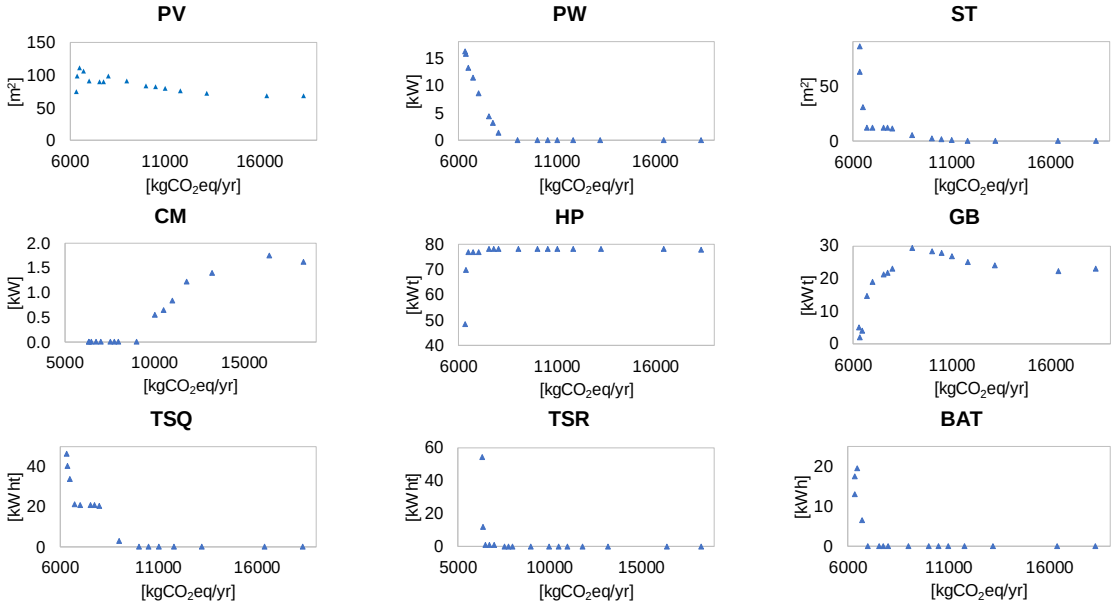

Fig. 3. Installed capacity along the Pareto curve for the grid connected system

Fig. 3 presents the technologies capacity with respect to the CO_2 emissions. ACH technology does not appear since it is not part of any configuration. As we can see PV, HP and GB technologies are feasible in every configuration. ST and PW technologies are only attractive when it is required a CO_2 emissions reduction higher than 55% with respect to the economic optimum. CM is viable above 12000 $kgCO_2eq/yr$, in which capacities above 1 kW is required. Although there is CM of 1 kW available in the market, this capacity is still very low, so it can be neglected in the trade off solutions. TSQ is viable below 9000 $kgCO_2eq/yr$ whereas TSR and BAT are feasible only close to the environmental optimum.

Fig. 4 shows the Pareto curve of the standalone system. Along the Pareto curve different solutions are obtained with different configurations and capacities. Each symbol corresponds to specific configuration (with different components and capacities). In this case, two Pareto curves are depicted corresponding to both battery technologies evaluated. As we can see the Pareto curves for both technologies are practically the same, however, the configurations do not coincide in every point necessarily.

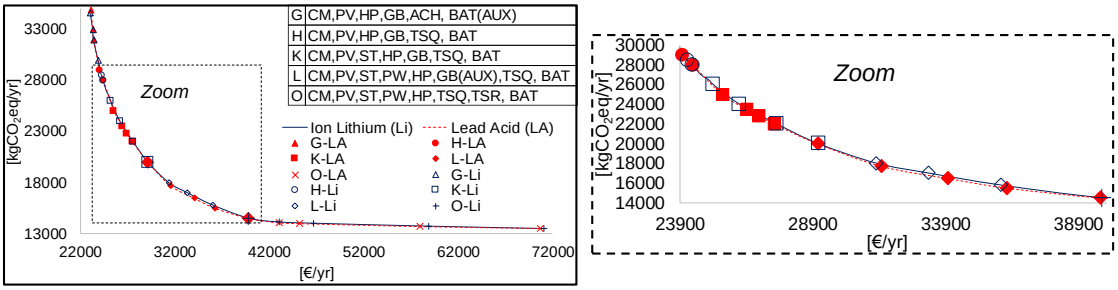

Fig. 4. Standalone system Pareto curve. Ion lithium (Blue-continuous) and Lead acid (Red-dashed) batteries

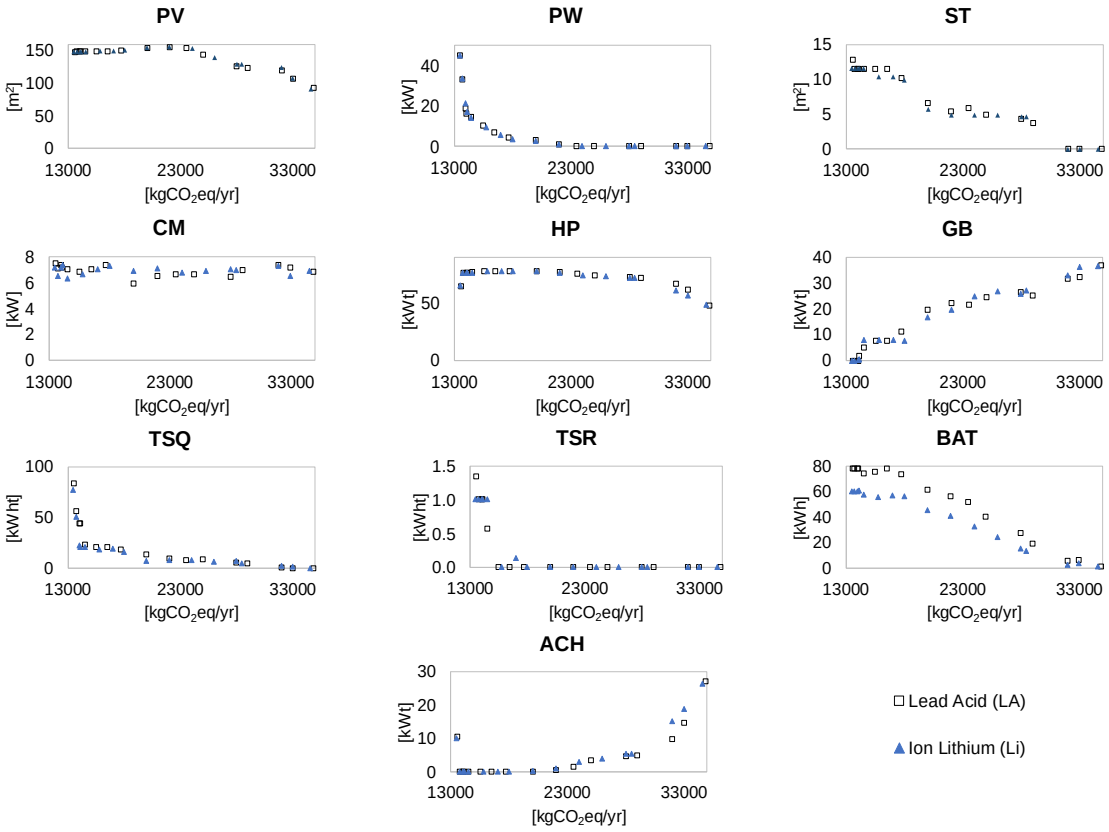

Fig. 5. Installed capacity along the Pareto curve for the standalone system

In this case, authors suggest the configurations H and K as interesting trade-off solutions. The difference between them lies only in the presence of ST in the K configuration. In H configuration it is possible to achieve a CO_2 emissions reduction of about 18% by increasing the annual cost in about 6%, whereas, through K configuration it is possible to achieve a CO_2 emissions reduction of about 25% up to 40% by increasing the annual cost in about 10% up to 20%, with respect to the economic optimum.

In the standalone system CM is the prime mover, therefore it is present in every configuration. From the Fig. 5 we can see that PV and HP technologies are feasible in every configuration. ST and PW technologies are present below about 26000 and 18000 $kgCO_2eq/yr$ respectively. ACH is part only in the configuration G which is above 32000 $kgCO_2eq/yr$. GB is present in G, H, K and L configurations, however, in this last could be considered as an auxiliary component (AUX) because its capacity decreases below the minimal commercial capacity up to disappearing in the configuration O. Regarding the electrical energy storage, we can see the difference in capacity between Ion Lithium and Lead acid batteries. Remark that smaller capacities are required for ion lithium technology to achieve the same relation €/$kgCO_2eq$ through the Pareto curve. In the economic optimum a small capacity is required in both cases, hence, it is considered that in the configuration G batteries are required as backup or auxiliary component (AUX) in the system. In the case of thermal storage, it is observed that TSQ is considered every configuration except in G configuration, whereas TSR is only considered in the O configuration close to the environmental optimum.

5. Conclusions

A multiobjective optimization was carried out to tackle the issue of conflicting objectives in the synthesis of polygeneration systems including renewable energy namely PV, ST and PW technologies, thermal energy storage and batteries. To this propose, a MILP model was developed and applied to a residential building located in Zaragoza (Spain) in two cases: Grid connected and Standalone. At first, representative days were selected to reproduce in a reasonable way the whole year data, reducing the computational effort during the optimization of the polygeneration system. Then, single optimizations were compared with respect to the reference systems, which show the advantages of using polygeneration systems with respect to the conventional systems from the economic and environmental point of view. The ε-constraint method was applied to obtain the Pareto curve or trade off solutions. Five different configurations were defined through the Pareto curve according to the minimum commercial capacities available in the market which allow different €/kgCO_2eq ratios. Interesting solutions show that a CO_2 emissions reduction of about 43% with only an increasing of about 7% in the total annual cost could be achieved in the grid connected system, whereas in the standalone system a CO_2 emissions reduction of about 18% could be achieved by increasing the annual cost in about 6%. In every case PV and HP technologies are feasible from the economic and environmental point of view for both systems. Regarding energy storage, in the grid connected system, TSQ become important only from about 50% of CO_2 emissions reduction, whereas TSR and batteries are considered only close to the environmental optimum. On the other hand, in the standalone system, TSQ and batteries become important from about 12% of CO_2 emissions reduction, whereas TSR is considered only close to the environmental optimum.

Acknowledgements

This work was developed in the frame of the research projects ENE2014-57262-R and ENE2017-87711-R, partially funded by the Spanish Government (Energy Program), the Government of Aragon (Spain) and the EU Social Fund (FEDER Program). The authors also want to acknowledge the mobility program for Latin-Americans offered by Unizar-Santander Universities.

References

AENOR, 2005. Instalaciones solares térmicas para producción de agua caliente sanitaria-UNE 94.002.

Ardani, K., O'Shaughnessy, E., Fu, R., McClurg, C., Huneycutt, J., Margolis, R., 2016. Installed Cost Benchmarks and Deployment Barriers for Residential Solar Photovoltaics with Energy Storage: Q1 2016.

Atersa, 2017. Specifications of photovoltaic module A-255P [WWW Document]. URL http://www.atersa.com/Common/pdf/atersa/manuales-usuario/modulos-fotovoltaicos/Ficha_Tecnica_A-255P-A-265P_Ultra.pdf (accessed 1.6.18).

BAXI, 2017. Catálogo tarifa [WWW Document]. URL https://www.baxi.es/-/media/websites/baxies/files/catalogo-2017-bajaress.pdf (accessed 1.6.18).

Beccali, M., Cellura, M., Longo, S., Mugnier, D., 2016. A Simplified LCA Tool for Solar Heating and Cooling Systems. Energy Procedia 91, 317–324. https://doi.org/10.1016/J.EGYPRO.2016.06.226

Bornay, 2017. Wind turbine specifications [WWW Document]. URL https://www.bornay.com/es/productos/aerogeneradores/bornay (accessed 1.6.18).

Cho, J., Jeong, S., Kim, Y., 2015. Commercial and research battery technologies for electrical energy storage applications. Prog. Energy Combust. Sci. 48, 84–101. https://doi.org/10.1016/j.pecs.2015.01.002

Darrow, K., Tidball, R., Wang, J., Hampson, A., 2017. Catalog of CHP technologies.

DiOrio, N., Dobos, A., Janzou, S., Nelson, A., Lundstrom, B., 2015. Technoeconomic Modeling of Battery Energy Storage in SAM.

Domínguez-Muñoz, F., Cejudo-López, J.M., Carrillo-Andrés, A., Gallardo-Salazar, M., 2011. Selection of typical demand days for CHP optimization. Energy Build. 43, 3036–3043. Duffie, J.A., Beckman, W.A., 2013. Solar Engineering of Thermal Processes, 4th ed. John Wiley & Sons.

Dufo-López, R., Lujano-Rojas, J.M., Bernal-Agustín, J.L., 2014. Comparison of different lead–acid battery lifetime prediction models for use in simulation of stand-alone photovoltaic systems. Appl. Energy 115, 242–253. https://doi.org/10.1016/j.apenergy.2013.11.021

Endesa, 2017. Tarifas de energía Endesa [WWW Document]. URL https://www.endesaclientes.com/empresas.html (accessed 1.6.18).

ENERTRES, 2017. Catálogo tarifa 10E [WWW Document]. URL http://www.enertres.com/uploads/[1485867548]Tarifa-bomba-de-calor-2017-web.pdf (accessed 1.6.18).

Eurostat, 2017. Gas prices for household consumers [WWW Document]. URL http://appsso.eurostat.ec.europa.eu/nui/show.do?dataset=nrg_pc_202&lang=en

Frischknecht, R., Itten, R., Sinha, P., Wild-Scholten, M. de, Zhang, J., 2015. Life Cycle Inventories and Life

Cycle Assessments of Photovoltaic Systems.
Fthenakis, V., Raugei, M., 2017. 7 – Environmental life-cycle assessment of photovoltaic systems. Perform. Photovolt. Syst. 209–232. https://doi.org/10.1016/B978-1-78242-336-2.00007-0
Fu, R., Feldman, D., Margolis, R., Woodhouse, M., Ardani, K., 2017. U.S. Solar Photovoltaic System Cost Benchmark: Q1 2017.
Guadalfajara, M., 2016. Economic and environmental analysis of central solar heating plants with seasonal storage for the residential sector. Universidad de Zaragoza.
Haimes, Y.Y., Lasdon, L.S., Wismer, D.A., 1971. On a bicriterion formation of the problems of integrated system identification and system optimization. IEEE Trans. Syst. Man. Cybern. 3, 296–297.
Hiremath, Mitavachan & Derendorf, Karen & Vogt, T., 2015. Comparative Life Cycle Assessment of Battery Storage Systems for Stationary Applications. Environ. Sci. Technol. https://doi.org/10.1021/es504572q
Homer Energy, 2016. HOMER® Pro Version 3.7 User Manual.
IDAE, 2017. Código Técnico de la Edificación-Ahorro de energía.
IDAE, 2016. Factores de emisión de CO2 y coeficientes de paso de energía primaria de diferentes fuentes de energía final consumidas en el sector de edificios en España.
IDAE, 2011a. Consumos del Sector Residencial en España - Resumen de Información Básica.
IDAE, 2011b. Pliego de Condiciones Técnicas de Instalaciones Conectadas a Red.
IDAE, 2011c. Plan de Energías Renovables (PER) 2011-2020.
IDAE, 2009. Escala de calificación energética para edificios de nueva construcción.
ISSF, 2015. Stainless Steel and CO2 : Facts and Scientific Observations.
JUDELSA, 2017. Energética futura-Tarifa de productos [WWW Document]. URL https://energeticafutura.com/recursos/documentos/tarifa.pdf (accessed 1.6.18).
LINDO Systems Inc, 2013. Lingo-Optimization Modeling Software for Linear, Nonlinear, and Integer Programming.
Mancarella, P., 2014. MES (multi-energy systems): An overview of concepts and evaluation models. Energy 65, 1–17. https://doi.org/10.1016/J.ENERGY.2013.10.041
Manwell, J.F., McGowan, J.G., 1993. Lead acid battery storage model for hybrid energy systems. Sol. Energy 50, 399–405. https://doi.org/10.1016/0038-092X(93)90060-2
Manwell, J.F., McGowan, J.G., Rogers, A.L., 2009. Wind Energy Explained, 2nd ed. WILEY.
Marín-Giménez, J.M., 2004. Evaluación de alternativas para el abastecimiento energético de una urbanización residencial en Zaragoza.
McManus, M.C., 2012. Environmental consequences of the use of batteries in low carbon systems: The impact of battery production. Appl. Energy 93, 288–295. https://doi.org/10.1016/J.APENERGY.2011.12.062
Meteotest, 2017. Meteonorm Software.
Orrell, A., Poehlman, E., 2017. Benchmarking U.S. Small Wind Costs With the Distributed Wind Taxonomy.
Parra, D., Swierczynski, M., Stroe, D.I., Norman, S.A., Abdon, A., Worlitschek, J., O'Doherty, T., Rodrigues, L., Gillott, M., Zhang, X., Bauer, C., Patel, M.K., 2017. An interdisciplinary review of energy storage for communities: Challenges and perspectives. Renew. Sustain. Energy Rev. 79, 730–749.
Peters, J.F., Baumann, M., Zimmermann, B., Braun, J., Weil, M., 2017. The environmental impact of Li-Ion batteries and the role of key parameters – A review. Renew. Sustain. Energy Rev. 67, 491–506.
Pina, E.A., Lozano, M.A., Serra, L.M., 2017. A Multicriteria Approach for the Integration of Renewable Energy Technologies and Thermal Energy Storage to Support Building Trigeneration Systems, in: International Confenerence on Solar Heating and Cooling for Buildings and Industry.
Poncelet, K., H. H oschle, Delarue, E., Virag, A., W.D'haeseleer, 2017. Selecting representative days for capturing the implications of integrating intermittent renewables in generation expansion planning problems. IEEE Trans. POWER Syst. 32. https://doi.org/10.1109/TPWRS.2016.2596803
Ramos, J., 2012. Optimización del diseño y operación de sistemas de cogeneración para el sector residencial comercial. Universidad de Zaragoza.
Red Electrica de España, 2017. Demanda y producción en tiempo real [WWW Document]. URL http://www.ree.es/es/actividades/demanda-y-produccion-en-tiempo-real
Salvador Escoda S.A, 2017. Tarifa de precios [WWW Document]. URL http://www.salvadorescoda.com/tarifas/index.htm (accessed 1.6.18).
Tapia-Ahumada, K., Pérez-Arriaga, I.J., Moniz, E.J., 2013. A methodology for understanding the impacts of large-scale penetration of micro-combined heat and power. Energy Policy 61, 496–512.
Tremeac, B., Meunier, F., 2009. Life cycle analysis of 4.5 MW and 250 W wind turbines. Renew. Sustain. Energy Rev. 13, 2104–2110. https://doi.org/10.1016/J.RSER.2009.01.001
U.S. Department of Energy, 2017. Absorption Chillers for CHP Systems.
Valor, E., Meneu, V., Caselles, V., 2001. Daily air temperature and electricity load in Spain. J. Appl. Meteorol. 40, 1413–1421.
Viti, A., 1996. Preparación de agua caliente para usos sanitarios.
Wakui, T., Yokoyama, R., 2015. Optimal structural design of residential cogeneration systems with battery based on improved solution method for mixed-integer linear programming. Energy 84, 106–120.